ANALYSIS OF NEW HIGH-Q_0 SRF CAVITY TESTS BY NITROGEN GAS DOPING AT JEFFERSON LAB*

A. D. Palczewski[†], R. L. Geng, and C. E. Reece

Thomas Jefferson National Accelerator Facility, Newport News, VA 23606, USA

Abstract

In order to refine systematic understanding and establish confident process control, Jefferson Lab has joined with partners to investigate and thoroughly characterize the dramatically higher Q_0 of 1.3 GHz niobium cavities first reported by FNAL in 2013[1]. With partial support from the LCLS-II project, JLab has undertaken a parametric study of nitrogen doping in vacuum furnace at 800 °C followed by variable depth surface removal in the 5 - 20 µm range. Q_0 above 3×10^{10} are typical at 2.0 K and 16 MV/m accelerating field. We report observations from the single cell study and current interpretations. In addition to the parametric single cell study, we also report on the ongoing serial testing of six nitrogen-doped 9-cell cavities as baseline prototypes for LCLS-II.

INTRODUCTION

JLab is collaborating with FNAL and Cornell to expedite the development and exploitation of methods to produce dramatically lower-loss SRF cavities using the nitrogen doping technique discovered by FNAL[2-6]. The LCLS-II project[7] is eager to take advantage of these developments to minimize cryogenic capital and operating costs. JLab's contribution to this effort centers on systematic processing and test of a set of single-cell 1.3 GHz cavities, followed by a "production-style" run treating six existing new TESLA-style 9-cell cavities to assess any performance and yield issues.

The envisioned parametric study included two rounds of matrix testing of 9 single cell cavity where the exposure to nitrogen would be held constant in each round and the post nitrogen annealing time and electropolishing (EP) would be varied. This matrix was performed twice; first with a 2 min exposure of nitrogen with 5, 10 and 15 µm EP removal and second with 20 min exposure with 10, 15 and 20 µm EP removal. These two sets of data along with auxiliary side tests would be performed before a fixed-recipe serial test of six 9-cell cavities in order to understand the yield associated with integrating N doping into a standard production process.

To date, Jefferson Lab has performed over 25 nitrogen doping/EP cycles on 18 SRF cavities and 30 vertical cryogenic tests including cavities outside the LCLS-II funded scope [8]. The matrixed studies showed the ability to dope an SRF cavity and control the EP removal to gain a lower BCS resistance and create a cavity which has a rising Q_0 with gradient is straightforward and easier than

initially envisioned. We have found with any doping used at ~25 mTorr, the EP window is over 15 µm wide which yields $Q_0 \geq 3.3\times10^{10}$ performance of the 1.3 GHz cavities at E_{acc} = 16 MV/m at 2.0 K.

The unforeseen complications within the systematic study turned out not to be within the doping or subsequent EP removal, but rather controlling the environmental conditions, both cooling profiles (spacial thermal gradients) and remnant magnetic fields to not mask the improvements due to nitrogen doping.

800°C HEAT TREATMENT – NITROGEN ABSORPTION

To date there have been over 60 cavities nitrogen doped at FNAL, JLab and Cornell combined. All the doping consists of about the same procedure with any minor changes coming from the nitrogen injection systems. The heat treatments begin with a standard ILC/XFEL 800 °C heat treatment for three hours to remove hydrogen from the bulk, followed by addition of low pressure nitrogen ~20 mTorr and a nitrogen diffusion period. For the six 9-cell LCLS-II baseline testing cavities, the JLab doping was decided to be an 800°C anneal for three hours, a 20-minute nitrogen doping with a controller set point of 20 mTorr (26 mTorr average pressure) with no active pumping and a 30-minute anneal after pumping out the nitrogen. The nomenclature for the doping is 800°C_A180_N20@26mTorr_A30. Including the ramp up and cooldown, the full cycle time for a 9-cell nitrogen doping run is approximately 18 hours (This includes the vacuum pump-down time). During the nitrogen injection all vacuum valves are closed and the nitrogen is injected through a 0.2 L/min orifice with a computer-controlled Brooks 4850 mass flow controller with feedback from the furnace convectron. An example of the temperature profile (red curve) and furnace pressure (blue curve) are shown in Fig. 1.

During doping, nitrogen gas is injected into the furnace until the set point is reached; because of the relatively high flow of the controller and long piping lengths, the controller overshoots the set point by approximately 10 mTorr. The valve closes and the cavity absorbs the N_2 until the pressure drops below the set point. At this time the flow is turned back on. This creates asymmetric saw-tooth in the furnace pressure (Fig. 2, red curve) with short pulses of gas (Fig. 2, black curve). This injection and decay profile (dp/dt) allows us to calculate the absorption rate (Fig. 2, blue curve) as well as the total amount of nitrogen absorbed by the cavity. This is illustrated in Fig. 2 for the 20 minute nitrogen injection of AES031 – 9 cell TESLA-shaped cavity. Using the flow from the

calibrated controller or the Δp/Δt calculation, we have found the amount of nitrogen absorbed is ~150 standard torr-liters of N_2. Using the same analysis on the two-minute doping for single cell cavities, the absorbed amount was ~10 torr-liters of N_2.
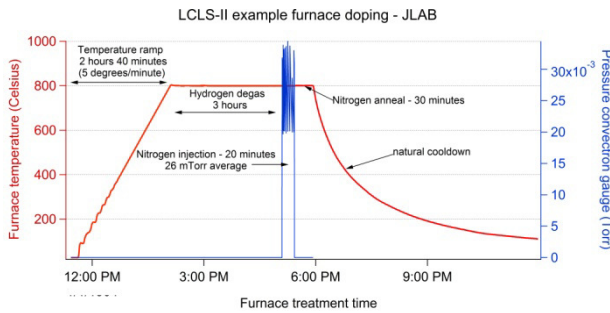

Figure 1: Example furnace data for 9-cell heat treatment. Red curve is the temperature profile and the blue curve is the convectron gauge data on the furnace used to see nitrogen during injection.
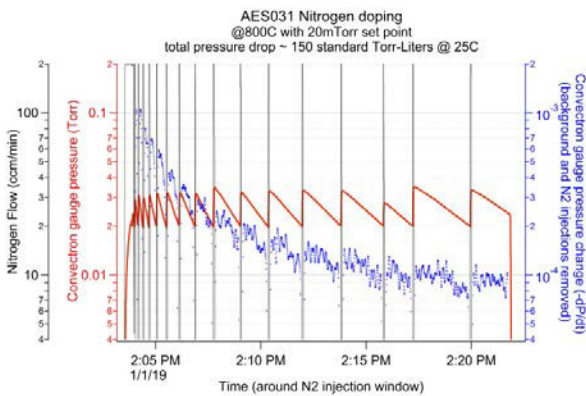

Figure 2: Nitrogen doping of AES031 with absorption rate and nitrogen flow.

TESTING ENVIRONMENT AND RF SURFACE RESISTANCE

During the first round of single cell doping there was a large discrepancy between the residual resistance of cavities tested in JLab's dewar 7 (D7) and dewar 8 (D8); where dewar 7 testing regularly produced nitrogen-doped cavities with a residual resistant below 2 nΩ (Q_0 greater than 1×10^{11} @ 1.5 K) while D8 produced residual resistance on the order of 7 nΩ (Q_0 less than 4×10^{10} at 1.5 K). This systematic effect was not recognized until after the cavities were reprocessed with a different doping. To test the effect of the change in testing environment, we took the high-Q_0 nitrogen-doped single cell cavity RDT-15 and RF tested it in both D7 and D8 without any processing between the tests. The tests results at both 2.0 K and 1.5 K are shown below in Fig. 3 with the solid symbols. In addition, the temperature data from D7 test from 2.1 K, 1.9 K, 1.8 K, 1.7 K, and 1.6 K are also shown in the open symbols. The residual resistance changed from less than ~2 nΩ at 14 MV/m in D7 to ~ 9 nΩ @14M/m in D8. Subsequent analysis

attributes the change to a combination of increased magnetic field and very uniform cavity cooling due to cryogen flow conditions in D8.
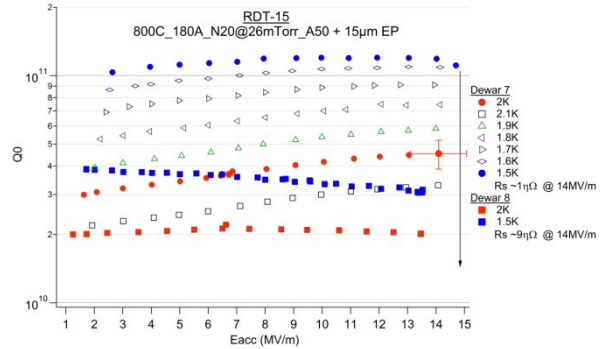

Figure 3: Dewar environment swap test RDT-15.

In view of recent new theoretical treatments of the field and temperature dependence of BCS-derived effective RF surface resistance, $R_s(B_{pk},T)$,[9, 10] we compare this data from RDT-15 with such calculations in the limit of equilibrium quasiparticle distributions, and find good agreement with the hypothesis that N-doping yielded a material with electron mean free path (mfp) of 10 nm and superconducting material parameters matching the standard text book ones for niobium[11-13]. Addition of a field- and temperature-independent residual resistance of 1.9 nΩ then predicts the experimental data from the D7 test in Fig. 3. These data and theoretical calculations are presented together in Fig. 4. Further analysis continues.
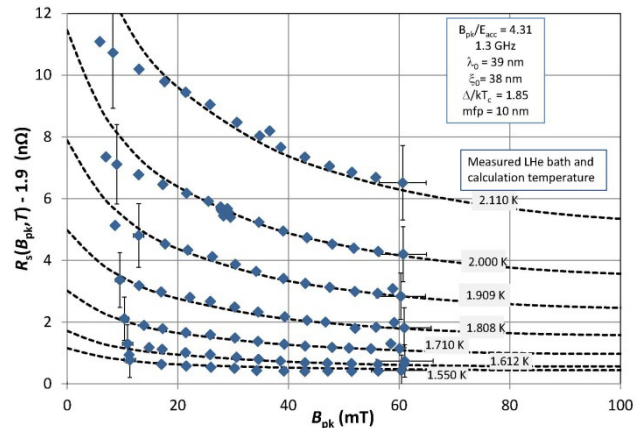

Figure 4: $R_s(B_{pk},T)$ from the cavity test in Figure 3 and corresponding Nb prediction by Xiao code [9] with mfp of 10 nm.

Q_0 DROP FROM QUENCHING

At 2.0 K the total surface resistance of nitrogen-doped cavities can be lower than 5 nΩ; this may compared to a "standard" cavity where the total resistance is closer to 15 nΩ. In consequence a small change in the resistance from magnetic flux trapped following a quench can lower the Q_0 by a significant fraction. To date we have seen cavities which quench 100's of times with no change in the resistance, while others have large changes following a single quench event. A dramatic example is shown in

Fig. 5 on RDT-5 which was doped with an 800°C_A180_N2@40mTorr_A6 recipe and then received a 5 µm EP. The change in the total resistance from a single quench was 7 nΩ, yielding a Q change from 5×10^{10} to 2.2×10^{10} @ 2.0 K. Thermal cycling to 200 K and re-test returned the Q_0 to its original value.
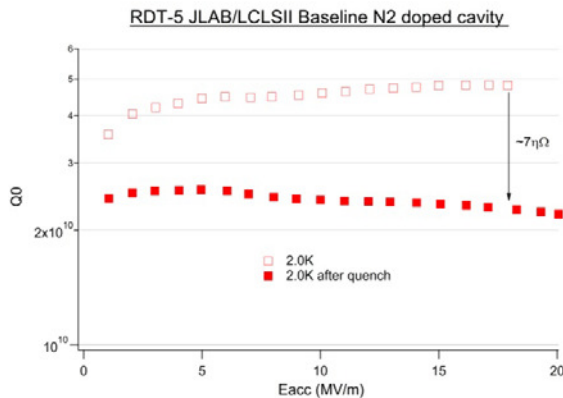

Figure 5: 2.0 K test of RDT-5 before and after Q_0 drop from quench. Thermal cycling to 200 K returned the Q_0 to its original value – not shown.

IN-SITU COOLDOWN INSTRUMENTATION – 9 CELL TESTING

During the vertical test of each 9-cell TESLA-style 1.3 GHz prototype cavity the remnant field as well as cooling rate is logged for each test. Thermal sensors (Lakeshore - Cernox CX-1050-SD-HT-1.4L) are located on each end flange, on the top side of cells 1, 3, 7, and 9 and two sensors on the top and bottom of cell 5 to track the temperature gradient across the high field location of the cell. In addition to the Cernox, there were also six Bartington single axis flux gate magnetometers (MAG-F) attached to the outside of the cavity at equator edges to track fields while the cavity cools. Four flux-gates were mounted looking up along the Z direction (cylindrical axis), one at the bottom of the cavity, and one on cells 1, 5, and 9; there was also one in the radial-direction facing the cavity and one placed orthogonal, looking tangentially to the cavity equator on cell 5. All sensors were aligned to the plane of the input coupler except for the flange sensors which were on the center of the cavity axis. The data acquired on select sensors during the cooldown of AES033 are depicted in Fig. 6. One can see the temperature between the top and bottom flanges is ~140 K and the temperature gradient across cell 5 (two red curves) is 5 K (about 10 cm vertical spacing) at the start of the cavity transition through T_c. There are clear signs of thermal gradient effect on the magnetic field where the field on cell 1 changes drastically as the cavity cools and flux expulsion where the cavity goes through T_c and the magnetic field jump. The nuances of the thermal gradient magnetic field and expelled flux are currently under investigation.
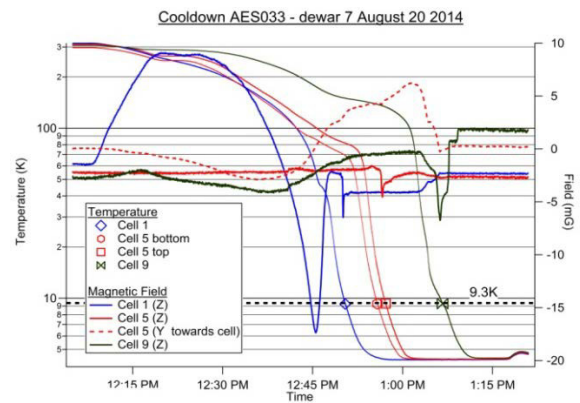

Figure 6: Cooldown data from AES033 in dewar 7.

9-CELL RF RESULTS WITH FROZEN PROTOCOL

To date we have tested three of the six 9-cell cavities with a frozen serial testing recipe. All cavities received 115 µm bulk EP regulated at 20°C in the style of the CEBAF 12 GeV upgrade production[14], followed by nitrogen doping (800°C_A180_N20@26mTorr_A30) and 15 µm EP. Ultrasonic thickness measurements indicated material removal uniformity on cavity cells better than ~20%. The 2.0 K RF test results are shown in Fig. 7.

All cavities showed characteristic rising Q_0 with gradient, but Q_0 from AES032 in D8 is lower than expected. The cooldown in D8 was half the rate and the temperature deltas across the cavity between the bottom and top cell were ~ 3 kelvins vs. ~150 kelvins across AES031 and AES033 in D7 at the start of T_c transition. Cavities AES031, AES032, and AES033 quenched at 18 MV/m, 17.3 MV/m and 16.4 MV/m, respectively. For the AES032 test there was a small amount of field emission-induced radiation starting at 15 MV/m which seems to have dropped the Q_0 slightly. The other two tests showed no signs of field emission.
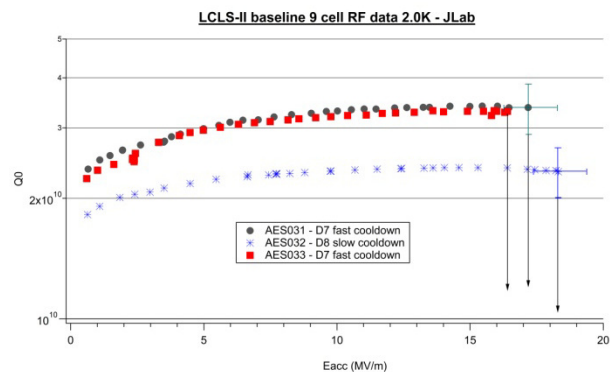

Figure 7: RF results for N doped 9 cell cavities.

ACKNOWLEDGEMENTS

REFERENCES

[1] A. Grassellino, *et al.*, Superconductor Science and Technology, 2013. **26**(10): p. 102001.

[2] A. Romanenko, *Breakthrough technology for very high quality factors in SCRF cavities*, in *LINAC14, these proceedings* 2014: Geneva. TUIOC02.

[3] D. Gonnella, *et al.* in *Proc. Int. Part. Accel. Conf. 2014*. 2014. Dresden, Germany: WEPRI064.

[4] A. Crawford, *et al.* in *Proc. Int. Part. Accel. Conf. 2014*. 2014. Dresden, Germany: WEPRI062.

[5] A. Romanenko, *et al.*, Journal of Applied Physics, 2014. **115**(18): p. 184903-184903-7.

[6] D. Gonnella, *et al.*, *Nitrogen-Treated Cavity Testing at Cornell*, in *LINAC14, these proceedings* 2014: Geneva. THPP016.

[7] J. Galayda, *The New LCLS-II Project Status and Challenges*, in *LINAC14, these proceedings* 2014: Geneva. TUIOA04.

[8] P. Dhakal, *et al.*, *Enhancement in Quality Factor of SRF Niobium Cavities by Material Diffusion*, in *Applied Superconductivity Conference* 2014: Charolotte, NC.

[9] B. P. Xiao, *et al.*, Physica C: Superconductivity, 2013. **490**(0): p. 26-31.

[10] A. Gurevich, PRL, 2014. **113**(8): p. 087001.

[11] V. Novotny, *et al.*, Journal of Low Temperature Physics, 1975. **18**(1-2): p. 147-157.

[12] R. D. Parks, *Superconductivity* 1969, New York: Dekker.

[13] C. Kittel, *Introduction to Solid State Physics* 1996: Wiley.

[14] C. E. Reece, *et al.* in *Proc. XXV Linear Accel. Conf.* 2010. Tsukuba, Japan: p. 779-781.